

Synthesis of single-crystalline nanobelts of ternary bismuth oxide bromide with different compositions

Junwei Wang and Yadong Li*

Department of Chemistry and the Key Laboratory of Atomic and Molecular Nanosciences (Ministry of Education), Tsinghua University, Beijing, 100084, P. R. China. E-mail: ydli@tsinghua.edu.cn

Received (in Cambridge, UK) 4th June 2003, Accepted 24th July 2003

First published as an Advance Article on the web 5th August 2003

Ternary bismuth oxide bromide nanobelts have been prepared by using the cationic surfactant cetyltrimethylammonium bromide (CTAB) as the bromine source; their composition can be easily controlled by changing the reaction conditions.

One-dimensional (1D) nanostructures have been the focus of extensive research over the past decade due to their unique electrical and optical properties and potential application in nanotechnology.^{1–3} A number of 1D nanostructures, such as nanoscale tubes, wires, rods and belts, were successfully fabricated, and a large part of this work has been concentrated on mono- and binary component structures, such as metals,⁴ oxides^{5–7} and II–VI,⁸ III–V^{9,10} compounds, *etc.* However, only limited kinds of single crystal ternary 1D nanostructures have been obtained until now, and the synthesis of new-type multi-component 1D nanostructures remains as a challenge to materials scientists.^{11–13} Here, we demonstrate that nanobelts of ternary bismuth oxybromide $\text{Bi}_{12}\text{O}_{17}\text{Br}_2$, $\text{Bi}_{24}\text{O}_{31}\text{Br}_{10}$, and $\text{Bi}_3\text{O}_4\text{Br}$ can be selectively prepared through a facile solution-based hydrothermal method using CTAB as the bromine source.

Binary and ternary bismuth oxides have been investigated as ionic conductors, catalysts, ferroelectrics and high-temperature superconductors.¹⁴ Oxyhalides are also an important family of compounds, which shows unique and excellent properties in electrical, magnetic, optical, and luminescent regimes.¹⁵ Bismuth oxyhalide has been used as a catalyst¹⁶ or for its therapeutic effects against microscopic carcinoma,¹⁷ and its activities may be enhanced using ultrathin nanobelts of bismuth oxyhalide because of their large surface-to-volume ratios.

Nanobelts of ternary bismuth oxybromide are prepared through a hydrothermal route, the composition of which could be controlled by simply adjusting pH of the solution. Briefly, 0.05 mol analytical-grade bismuth nitride ($\text{Bi}(\text{NO}_3)_3 \cdot 5\text{H}_2\text{O}$) and 0.05 mol CTAB were put into distilled water at room temperature. The mixture was stirred for ten minutes and the pH value of the resulting solution was adjusted above 8 by addition of 1 M NaOH solution. The solution was then stirred vigorously for 1 h and transferred into a Teflon-lined stainless steel autoclave with a capacity of 50 ml. The autoclave was sealed and maintained at 160–180 °C for 12–24 h. After the reaction was completed, the resulting white solid product was collected by filtration, washed with large amounts of distilled water to remove all impurities such as NaNO_3 and CTAB, and then dried at 50 °C for 3 h.

X-ray diffraction (XRD) has been used to characterize the crystal structure of the as-obtained bismuth oxybromide nanobelts. Fig. 1a shows a typical XRD pattern of $\text{Bi}_{24}\text{O}_{31}\text{Br}_{10}$ nanobelts, and all the peaks could be readily indexed to a monoclinic phase with lattice constants comparable with the values given in JCPDS 72–1184. The XRD pattern of $\text{Bi}_{12}\text{O}_{17}\text{Br}_2$ nanobelts is displayed in Fig. 1b, and most of the peaks could be indexed to a tetragonal structure of bulk $\text{Bi}_{12}\text{O}_{17}\text{Br}_2$ with cell constants $a = 5.48$ and $c = 35.69$ Å (JCPDS 37–0701) although some peaks due to Bi_2O_3 impurity are also seen, while all the peaks in Fig. 1c could be indexed to a pure orthorhombic phase of $\text{Bi}_3\text{O}_4\text{Br}$ (JCPDS 84–0793). All

these XRD patterns indicate that three different ternary phases of bismuth oxide bromide have been successfully synthesized.

Transmission electron microscopy (TEM) has provided further insight into the morphologies and structure details of these bismuth oxybromide products. Fig. 2a gives the TEM image of a typical example of as-synthesized $\text{Bi}_{12}\text{O}_{17}\text{Br}_2$ nanobelts with uniform width of 100–300 nm and lengths up to several micrometres. Fig. 2b shows a high-resolution TEM image of a single-crystalline $\text{Bi}_{12}\text{O}_{17}\text{Br}_2$ nanobelt. The spacing of 0.30 nm between adjacent lattice planes corresponds to the distance between two (0012) crystal planes. The selected area electron diffraction (SAED) pattern (Fig. 2b inset) indicates that the nanobelts are single crystals, whose long axis corresponds to the $\langle 100 \rangle$ direction. Fig. 3a and b show typical TEM images of structurally uniform and single crystalline $\text{Bi}_{24}\text{O}_{31}\text{Br}_{10}$ and $\text{Bi}_3\text{O}_4\text{Br}$ nanobelts, respectively. These nanobelts are all very thin (10–20 nm) and of high aspect ratio.

Thorough elemental composition analysis of these nanobelts was performed by energy-dispersive X-ray analysis (EDXA) and revealed that these nanobelts contained only Bi, Br and O. Fig. 4 shows a typical EDXA spectrum recorded on an

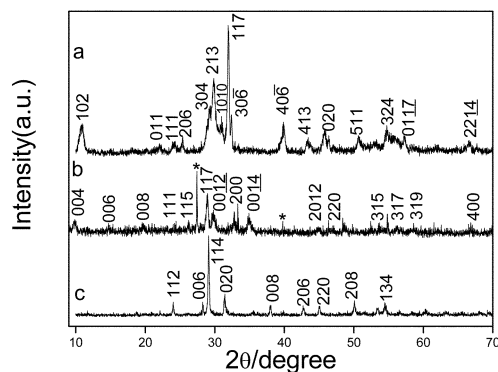


Fig. 1 XRD patterns of as-synthesized $\text{Bi}_{24}\text{O}_{31}\text{Br}_{10}$ (a), $\text{Bi}_{12}\text{O}_{17}\text{Br}_2$ (b), and $\text{Bi}_3\text{O}_4\text{Br}$ (c) nanobelts (*, peaks of Bi_2O_3).

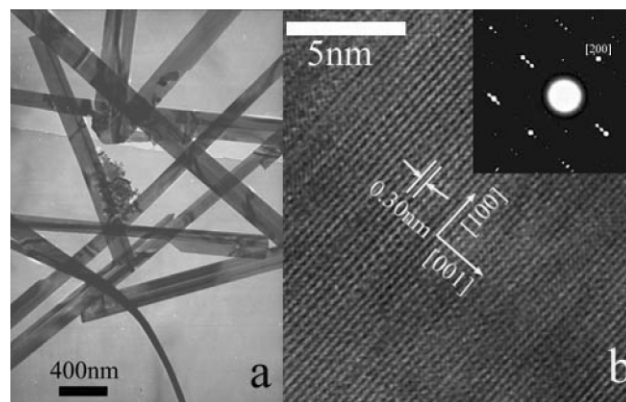


Fig. 2 (a) A typical TEM image of $\text{Bi}_{12}\text{O}_{17}\text{Br}_2$ nanobelts. (b) HRTEM image of a single $\text{Bi}_{12}\text{O}_{17}\text{Br}_2$ nanobelt. The inset is the corresponding SAED pattern.

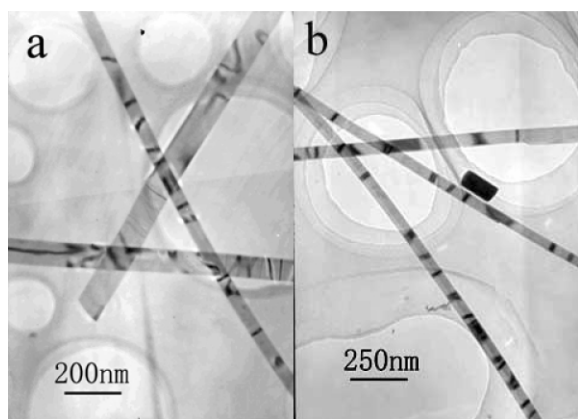


Fig. 3 Typical TEM images of (a) $\text{Bi}_{24}\text{O}_{31}\text{Br}_{10}$ and (b) $\text{Bi}_3\text{O}_4\text{Br}$ nanobelts.

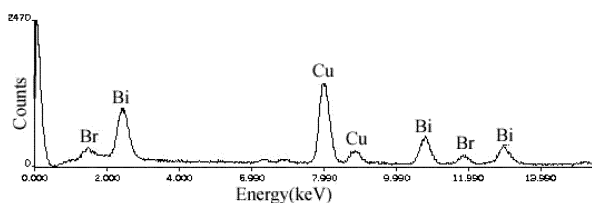


Fig. 4 EDXA spectrum of as-prepared $\text{Bi}_{12}\text{O}_{17}\text{Br}_2$ nanobelts.

individual $\text{Bi}_{12}\text{O}_{17}\text{Br}_2$ nanobelt, whose peaks are assigned to Bi and Br (the Cu peaks arise from the copper grid). Relative quantitative analysis shows that the atomic ratio of Bi to Br is 6.2.

We have demonstrated that various 1D nanostructures could be prepared by hydrothermal methods.^{7,13} For a solution-based process, reaction conditions, such as temperature and monomer concentration, play a key role in controlling the phase and anisotropic growth of crystals.^{18,19} In the current process, the controllable crystal phases and morphologies of bismuth oxybromide could be achieved by simply changing some growth parameters, including pH and temperature. Normally, we got $\text{Bi}_{24}\text{O}_{31}\text{Br}_{10}$ nanobelts at pH 8–10, $\text{Bi}_3\text{O}_4\text{Br}$ at 11–12, $\text{Bi}_{12}\text{O}_{17}\text{Br}_2$ at 13–14, but BiOBr nanoplates at lower pH (< 7) and Bi_2O_3 microstructures at higher base concentration in our synthetic conditions. In addition, due to the basic surroundings, Bi_2O_3 may be mixed in the product as a separate phase, and vigorous stirring before heating may avoid this. The optimal temperature for growth of the nanobelts is 160–180 °C. If the temperature is lower than this, thermodynamically stable nanoplates will be obtained. It is noteworthy that CTAB, as the bromine source, also determines the crystal structure and phase. Controlled experiments were conducted with CTAB replaced by NaBr, and only BiOBr nanoplates could be obtained whatever we changed pH at the same conditions. It is believed that the formation of CTA^+OH^- provides a proper environment for growth of bismuth oxide bromide nanobelts.

This present work shows that single-crystalline nanobelts of ternary bismuth oxide bromide $\text{Bi}_{12}\text{O}_{17}\text{Br}_2$, $\text{Bi}_{24}\text{O}_{31}\text{Br}_{10}$, and

$\text{Bi}_3\text{O}_4\text{Br}$ can be synthesized on a large scale by a facile solution-based hydrothermal method using CTAB as the bromine source. The phase and anisotropic growth of crystals are monitored by simply changing the reaction parameters based on a kinetically-driven process. CTAB also plays a unique role in controlling the phase and morphologies of bismuth oxide bromide. The synthetic method presented here may be extended to other 1D nanostructures of oxide bromide compounds by selecting the proper conditions.

This work was supported by NSFC (20025102, 50028201, 20151001), the Foundation for the Authors of National Excellent Doctoral Dissertations of P. R. China, and the state key project on fundamental research for nanomaterials and nanostructures.

Notes and references

- J. Hu, T. W. Odom and C. M. Lieber, *Acc. Chem. Res.*, 1999, **32**, 435.
- Y. Xia, P. Yang, Y. Sun, Y. Wu, B. Mayers, B. Gates, Y. Yin, F. Kim and H. Yan, *Adv. Mater.*, 2003, **15**, 353.
- M. H. Huang, S. Mao, H. Feick, H. Q. Yan, Y. Y. Wu, H. Kind, E. Weber, R. Russo and P. D. Yang, *Science*, 2001, **292**, 1897.
- Y. D. Li, J. Wang, Z. Deng, Y. Wu, X. Sun, D. Yu and P. Yang, *J. Am. Chem. Soc.*, 2001, **123**, 9904; Y. D. Li, X. L. Li, Z. X. Deng, B. C. Zhou, S. S. Fan, J. W. Wang and X. M. Sun, *Angew. Chem., Int. Ed.*, 2002, **41**, 333; J. W. Wang and Y. D. Li, *Adv. Mater.*, 2003, **15**, 445.
- R. Fan, Y. Y. Wu, D. Y. Li, M. Yue, A. Majumdar and P. Yang, *J. Am. Chem. Soc.*, 2003, **125**, 5254.
- Z. P. Pan, Z. R. Dai and Z. L. Wang, *Science*, 2001, **291**, 1947; Z. R. Dai, Z. P. Pan and Z. L. Wang, *J. Phys. Chem. B*, 2002, **106**, 902; Z. P. Pan, Z. R. Dai and Z. L. Wang, *Appl. Phys. Lett.*, 2002, **80**, 309.
- X. Wang and Y. D. Li, *Angew. Chem. Int. Ed.*, 2002, **41**, 4790; X. Wang and Y. D. Li, *J. Am. Chem. Soc.*, 2002, **124**, 2880; X. Wang and Y. D. Li, *Chem. Commun.*, 2002, **7**, 764; X. Wang and Y. D. Li, *Chem., Eur. J.*, 2003, **9**, 300; X. L. Li, J. F. Liu and Y. D. Li, *Inorg. Chem.*, 2003, **42**, 921; X. L. Li, J. F. Liu and Y. D. Li, *Appl. Phys. Lett.*, 2002, **81**, 4832.
- Z. X. Deng, L. B. Li and Y. D. Li, *Inorg. Chem.*, 2003, **42**, 2331; Y. D. Li, H. W. Liao, Y. Ding, Y. T. Qian, L. Yang and G. E. Zhou, *Chem. Mater.*, 1998, **10**, 2301; Y. D. Li, H. W. Liao, Y. Ding, Y. Fan, Y. Zhang and Y. T. Qian, *Inorg. Chem.*, 1999, **38**, 1382; Q. Peng, Y. J. Dong, Z. X. Deng and Y. D. Li, *Inorg. Chem.*, 2002, **41**, 5249.
- X. F. Duan and C. M. Lieber, *J. Am. Chem. Soc.*, 2000, **122**, 188; X. F. Duan and C. M. Lieber, *Adv. Mater.*, 2000, **12**, 298.
- J. Goldberger, R. R. He, Y. F. Zhang, S. W. Lee, H. Q. Yan, H. J. Choi and P. Yang, *Nature*, 2003, **422**, 599.
- J. J. Urban, W. S. Yun, Q. Gu and H. Park, *J. Am. Chem. Soc.*, 2002, **124**, 1186.
- J. A. Nelson and M. J. Wagner, *J. Am. Chem. Soc.*, 2003, **125**, 332.
- X. M. Sun, X. Chen and Y. D. Li, *Inorg. Chem.*, 2002, **41**, 4996.
- M. G. Francesconi, A. L. Kirbyshire, C. Greaves, O. Richard and G. Van Tendeloo, *Chem. Mater.*, 1998, **10**, 626.
- J. Lee, Q. Zhang and F. Saito, *J. Solid State Chem.*, 2001, **160**, 469.
- N. Kijima, K. Matano, M. Saito, T. Oikawa, T. Konishi, H. Yasuda, T. Sato and Y. Yoshimura, *Appl. Catal. A: Gen.*, 2001, **206**, 237.
- J. Rotmensch, J. L. Whitlock, M. L. Dietz, J. J. Hines, R. C. Reba, E. P. Horwitz and P. V. Harper, *Abstr. Pap. Am. Chem. Soc.*, 1998, **216**, 47–IEC Part 1.
- S.-M. Lee, Y. Jun, S.-N. Cho and J. Cheon, *J. Am. Chem. Soc.*, 2002, **124**, 11244.
- Z. A. Peng and X. G. Peng, *J. Am. Chem. Soc.*, 2002, **124**, 3343; Z. A. Peng and X. G. Peng, *J. Am. Chem. Soc.*, 2001, **123**, 1389.